9/2/14

Evaluating observation influence on regional water budgets in reanalyses

Michael G. Bosilovich * NASA/GSFC/GMAO
Jiundar Chern, Umd ESSIC
David Mocko, SAIC
Franklin R. Robertson, NASA MSFC
Arlindo M. da Silva, NASA GSFC GMAO

NASA/Global Modeling and Assimilation Office
Code 610.1 Goddard Space Flight Center
Greenbelt MD

Submitted to Journal of Climate

* *Corresponding address*: Global Modeling and Assimilation Office, Code 610.1 NASA Goddard Space Flight Center, Greenbelt, MD 20771, Michael.Bosilovich@nasa.gov

ABSTRACT

The assimilation of observations in reanalyses incurs the potential for the physical terms of budgets to be balanced by a term relating the fit of the observations relative to a forecast first guess analysis. This may indicate a limitation in the physical processes of the background model, or perhaps inconsistencies in the observing system and its assimilation. In the MERRA reanalysis, an area of long term moisture flux divergence over land has been identified over the Central United States. Here, we evaluate the water vapor budget in this region, taking advantage of two unique features of the MERRA diagnostic output; 1) a closed water budget that includes the analysis increment and 2) a gridded diagnostic output data set of the assimilated observations and their innovations (e.g. forecast departures).

In the Central United States, an anomaly occurs where the analysis adds water to the region, while precipitation decreases and moisture flux divergence increases. This is related more to a change in the observing system than to a deficiency in the model physical processes. MERRA's Gridded Innovations and Observations (GIO) data narrow the observations that influence this feature to the ATOVS and Aqua satellites during the 06Z and 18Z analysis cycles. Observing system experiments further narrow the instruments that affect the anomalous feature to AMSUA (mainly window channels) and AIRS. This effort also shows the complexities of the observing system, and the reactions of the regional water budgets in reanalyses to the assimilated observations.

1. Introduction

Critical evaluation of MERRA (Modern-Era Retrospective analysis for Research and Applications; see Appendix A for acronym definitions) global water and energy budgets has documented significant improvements in the annual mean spatial patterns and amounts of precipitation in NASA's latest reanalysis such that skill relative to GPCP / CMAP uncertainties is equivalent to that of the ECMWF-Interim reanalysis (Bosilovich et al. 2011). There are, nevertheless, areas where improvements can be made in the hydrologic and energy cycles of this reanalysis (and other contemporary reanalyses as well). For example, regional water cycles exhibit biases, and generally depend on the density and variability of observations available for assimilation. The extent of these problems can be deduced from the magnitude and behavior of the non-physical increment terms of state variable conservation equations (e.g. u, v, T, q). These increments provide a wealth of information as to the biases in model physics as well as the utility and veracity of the observations being assimilated. Bosilovich et al. (2011) and Robertson et al. (2011) show that (i) systematic regional biases in vertically-integrated moisture and heat budgets exist as manifestations of physics parameterization weaknesses, and (ii) these model biases interact with an evolving satellite observing system to cause spurious changes in fluxes produced by the assimilation.

For example, Trenberth et al. (2011) found that in MERRA and ECMWF Interim Reanalysis (ERA-I, Dee et al. 2011), atmospheric moisture divergence (which theoretically relates globally to evaporation (E) minus precipitation (P)) shows positive values over a substantial portion of the United States for a long time average. The land/atmosphere budget of water does not allow for continental E > P over long time periods, and so this result is not physical, sometimes called an imbalance. In a data assimilation system, this non-physical result is generated while numerically correcting the mass in the direction of observations over long periods of time. MERRA provides the analysis tendencies that can be used to diagnose closed budgets, but these tendencies represent the effect of the entire observing system at the analysis time. In order to better understand the source of these tendencies, it should be useful to evaluate the individual observing systems for 1) data availability and 2) which observing system is most closely related to the eventual analysis. While the impact of observational systems on analyses has been studied in respect to forecast error (e.g. Gelaro and Zhu 2009), here, we are focusing on the regional water vapor balance.

Figure 1 a and b show the moisture flux divergence (MFD) from MERRA and ERA-I (Dee et al. 2011) for the period 2001 – 2012. The positive MFD area over the central United States is a feature noted by Trenberth et al. (2011), who points out that there is no accounting of irrigation in the MERRA or ERA-I land parameterization. In the region where this anomalous divergence occurs, irrigation can make a contribution to surface evaporation (Ozdogan and Gutman 2008; Ozdogan et al. 2010). In evaluations of the central United States water cycle, lack of irrigation in the model may contribute to water vapor biases that the analysis should strive to overcome. However, it is not clear that the radiosonde network has enough data to close a regional water budget and then reconcile irrigation contributions to MFD (Yarosh et al. 1999; Kanamaru and Salvucci 2003). This comparison opens up numerous questions and is far from clear about the underlying causes of the imbalance. Is it seasonally varying? This is a short period in the MERRA record, does it hold for the 30 years? Are the imbalances in MERRA and ERA-I occurring for similar reasons? Since this is an unphysical result, it is likely related to the observational analysis. Which component(s) of the observing system contributes to this inconsistency? The objective of this study is to use some unique MERRA diagnostic output to better understand this feature and how it came to be present in the water cycle data.

2. Data

a. MERRA

MERRA is the first reanalysis produced at NASA since the early 1990s (more completely described by Rienecker et al. 2011). The objective of the project is to provide reanalysis data for the science community, but also to make some improvement of the water cycle beyond existing reanalyses. In November 2007, the GMAO completed a validation of the GEOS5 data assimilation system for MERRA, finding that the global total column water and precipitation exhibited spatial statistics better than existing (at that time) reanalyses, but spurious time variations of the mean water cycle were related to changes of the observational record. This is confirmed in the resulting MERRA data (Bosilovich et al. 2011), and at large scales MERRA is providing water cycle data better than the previous generation of reanalyses, and as good or better than the other most recent reanalyses. Of course, the water cycle still requires development in many areas.

The MERRA data assimilation system (GEOS5) also includes some unique attributes that affect the water cycle evaluation. The system uses a three dimensional variational assimilation scheme, but the model states are updated incrementally (Incremental Analysis Updates, IAU, as described by Bloom et al. 1996). While the IAU does significantly reduce shock of the analysis on precipitation, it also provides a tendency term in the moisture budget for the observational analysis.

$$\frac{\partial w}{\partial t} = -\nabla \cdot \overline{\left(\vec{V} w\right)} + (E - P) + \left[\frac{\partial w}{\partial t}\right]_{ANA} + F \quad (1)$$

The terms of the GEOS5/MERRA total vertically integrated atmospheric water budget are total water change, moisture flux divergence, surface evaporation (*E*), liquid and solid precipitation (*P*), the analysis tendency and a negative fill correction (*F*, typically less than 0.04% of precipitation or evaporation, global average). The vertical integration is performed during the cycling of the data on model native vertical coordinate. The analysis tendency term (derived from IAU discussed above, hereinafter referred to as ANA) originates with the observational analysis and provides a diagnostic value of the mean departure from observations (as an aggregate of all assimilated observations). In some studies that consider this influence on the water budget, the term was solved as a residual (e.g. Roads et al. 2002), but with MERRA the full water budget is produced, including vertically integrated quantities. A key point here is that the ANA term is not just a measure of imbalance, but has spatially and temporally varying structure related to the comparison of the background forecast model with the available observations.

b. Gridded Innovations and Observations (GIO)

The observations and forecast departures resulting from the data assimilation process are typically stored in observation-space formatted files, in that they have coordinates in space and time to their exact location, unique to each observation record. This level of spatiotemporal precision for data assimilation is required to make the best use of the observations and to diagnose the eventual analysis. However, the data formats can be more diverse than typical reanalysis output, and may vary depending on the instrument. Likewise, missing records can complicate evaluation. In order to more easily compare multiple instruments and observing systems, and simplify the data access, we have developed the Gridded Innovations and Observations (GIO) data set. Assimilated data are binned to the native MERRA analysis grid in space and time (2/3° longitude by ½° latitude, 42 levels and 6 hourly synoptic times), for each observing platform and observations type, as well as instrument and channel. The data files include the observation, the forecast departure (observation minus forecast, OmF), and analysis departure (observation minus analysis, OmA). If multiple observations from the same observing system are binned in the same grid space, they are averaged and the GIO files also include the data count and standard deviation in each bin.

While evaluating this particular gridded data, one must consider there are missing data and all grid points may not have the same number of binned observations. Instead, we must make use of both the observation value and the number of observations in a grid box. For example, monthly mean temperature (T) can be determined from 6-hourly binned temperature (T') by,

$$T = \sum_{t=1}^{M} T'(t) \times n(t) \Big/ \sum_{t=1}^{M} n(t). \qquad (2)$$

Where M is the number of 6-hourly analyses cycles in a month, and n is the number of observations that were used to create the binned temperature. Likewise, area averages must consider the total number of observations over the area. If the data were in observations space, then this is essentially how the average would be computed. The important point is that the gridded data include the number of observations that create the binned average, and considering the number of observations is important to appropriately average boxes with many observations and those with few. The advantage of gridded data is that the uniform file formats can be more easily evaluated in standard software, and file sizes are much smaller. Caution must still be exercised in that small numbers of observations or asymmetric distributions of observations may significantly affect time and space averaging.

Here, we refer to physical observations or retrieved satellite observations that are assimilated as "conventional" observations, distinguishing those from remotely sensed radiances (Rienecker et al. 2011). In data volume, the conventional observations are smaller than the radiance observations, and so are merged together in a single collection of different variables, whereas each assimilated channel's radiance observations are collected with its respective instrument (e.g. MSU, SSU, AMSU, HIRS and SSM/I) and satellite. Conventional observations with a vertical dimension (such as radiosondes) are likewise binned to MERRA's vertical grid (42 pressure levels). In general, gridding does provide a cost savings for the radiance data, as the spatial resolution can be very high, even if much of the globe is not observed during an assimilation cycle for a given instrument. Data distribution in space and time, relative to the region of interest will be discussed later in sections 3c and 3d.

c. MERRA-Land

Recognizing that the atmospheric forcing above the land surface can be biased due to atmospheric model biases, Reichle et al. (2011) developed MERRA-Land. This is a reprocessing of the land model parameterization (only), using bias corrected precipitation in place of the model-generated precipitation that provides the water source for land in MERRA. Other forcings are derived from MERRA. The bias correction ensures that at long periods, the MERRA-Land precipitation reflects observed values. In this way, we can also assess MERRA precipitation bias and any consequence that may have in the budget analysis, whereas MERRA-Land provides a comparison for P, E and E-P that we may expect to have some higher quality than MERRA itself.

3. Central United States

a. Vertically Integrated Water Cycle Climatology

The main purpose of this paper is to investigate the long-term moisture flux divergence (MFD) pointed out by Trenberth et al. (2011) and shown in Figure 1 a and b. This feature is not persistent throughout the period of the satellite era reanalyses (Figure 1 c and d). Considering the area average for the Central US (region demarcated by the red box in Figure 1a), the transition into excessive MFD is a jump in the regions time series (Figure 2). Interestingly, MERRA's transition occurs around 2000, while ERA-I (Dee et al. 2011) experiences a jump in 1994. This difference suggests that the underlying causes in each system are not comparable. The subsequent analysis focuses on MERRA because of this disparity in the time series and occurrences of the change, but also because MERRA includes more output diagnostics readily available than ERA-I. This temporal variation was not presented by Trenberth et al. (2011), but we will use the disparity between the years before and after 2001 to identify the impact and causes of the shift. In the subsequent evaluations, we considered that the shift may be related to a physical process (for example, sea surface temperature through teleconnections or lack of irrigation at the land surface) or assimilated data (type, quantity or quality), but ultimately, it becomes clear that observing system changes are a primary consideration.

Over long periods, terms for total tendency and corrections (F) can be neglected in equation 1. The remaining terms of the vertically integrated water balance are provided in Figure 3. The first noticeable comparison is that the analysis increment (ANA) pattern over land matches closely the MFD pattern, even in negative (converging) regions. The interactions with the surface are apparent as well, for example, the Great Lakes appear as a source of atmospheric water for divergence in E-P. However the sudden shift to positive analysis increments in 2000 seems to rule out a missing surface evaporative source causing the Central US positive MFD. There is not an obvious correlation between the Central US E, P or E-P and ANA, which suggests the water vapor being added through the analysis is contributing to MFD. Though, this is not to say that an appropriate accounting of irrigation in the reanalysis is unimportant.

For most of the 34-year period, MERRA precipitation is lower than MERRA-Land in the Central US (Figure 4a, keeping in mind that MERRA-Land precipitation is bias corrected by CPCU rainfall observation data). The evaporation in both data sets is strongly constrained by the precipitation, and MERRA Central US evaporation then should be underestimated. If we consider that, in a physical sense, E-P should be long-term moisture flux divergence, both MERRA and MERRA-Land E-P have similar interannual variability (Figure 4b). However, MERRA periods of negative E-P (convergence) seem to be somewhat weaker amplitude compared to those in MERRA-Land. It is also clear that MERRA E-P shows little resemblance to MFD interannual variability. The MFD interannual variability tracks very closely with the analysis increment, especially the strong shift around 2000 that leads to the divergent area in Figure 1 and Figure 3. To emphasize this, Table 1 shows correlations of the annual mean time series of the Central US MERRA water budget terms. The strongest interannual relationships seem to be between ANA and MFD, and also between P and E. Since there is no data assimilation in the land surface, at long time scales, E follows P leading to a high correlation. Given that precipitation exhibits a mean low bias against observations, it is puzzling that the precipitation is negatively correlated to ANA, so that the addition of water from the analysis is not contributing to increased precipitation.

Figure 5 compares the mean annual cycle of the vertically integrated water budget before and after the shift in the early 2000s. Despite substantial reductions in both E and P in more recent times, E-P remains stable across the shift, again, as E is limited by P in the land model. However, MFD and ANA increase substantially across the shift mainly during the warm and wet seasons (relative to atmospheric temperature and humidity) from spring through early fall, with differences peaking in July and August. The ANA increments are positive from June-September, adding water to the column, especially after the shift. The E-P mean annual cycle peaks in early summer, 1-2 months earlier than that of MFD and is substantially weaker than the latter. The additional water from ANA is contributing to the increase of MFD, but it is not intuitive as yet, why the precipitation should decrease. The total water tendencies are small, and do not change across the shift (not shown).

The mean diurnal cycle (for all seasons) is characterized in Figure 6, including the comparison around the 2001 shift. One feature worth explaining first is the ANA diurnal cycle. MERRA produces 4 analyses at each of 00Z, 06Z, 12Z and 18Z. This defines the analysis increment, which for an analysis time is determined over the previous 6h, is carried backward in time, and is used to determine the analysis tendency, termed ANA here, for the water budget in a separate model integration (this is called the assimilation cycle, more details are explained by Rienecker et al. 2011). The ANA tendency is fixed for the 6 hour assimilation cycle, and when plotted in an hourly diurnal cycle appears flat for each 6 hour period, and steps to the next time period. Before 2001, the mean 00Z and 12Z analysis increments are small, close to zero. After 2001, the 12Z analysis increments add water to the column, but 00Z increments remove water from the column. This systematic diurnal cycle of ANA after 2001 can be problematic, repeatedly adding water then removing it, will be detrimental to the regional water cycle. Before 2001, 18Z and 06Z each act to remove water from the system at a relatively low rate. The diurnal cycle of the ANA vertical profiles will be discussed further in the next section.

The reduction in precipitation after 2001 is spread across the diurnal cycle. Of course, evaporation is small at night, so the reductions in water stored in the surface mostly affect the daytime maximum of evaporation. There is a general increase of divergence across the diurnal cycle, with increased daytime divergence and less nighttime convergence after 2001. A substantial portion of the increased divergence occurs from 06Z through 15Z when the ANA term is adding water to the system. However, at any given hour of the mean diurnal cycle, the total tendency may also be non-zero. The ANA term affects first the water content as evidenced by the total tendency, then MFD catches up after some time. During the drier daytime (relative to surface evaporation, and smaller total positive change), the analysis increment is not adding water, but divergence is removing it from the region. If the analysis were working to compensate for low evaporation at the surface, the 18Z increment would be the most direct way to make that adjustment. Without radiosondes in the 18Z analysis, the increments are relying on remotely sensed observations. Satellite data will be considered in section 3d.

b. Three Dimensional Water Vapor Budget

While it is often convenient to study the vertically integrated water vapor budget, physical, dynamical and assimilation processes are occurring in three dimensions and so the vertical distribution of the tendencies can be important in understanding the budget. Figure 7 compares the vertical section of main terms of equation 1 with annual area averages for the central US region. Here, MST represents the moist precipitation processes (condensation and rain evaporation) while TRB represents the turbulent tendencies (which vertically integrates to surface evaporation). Note that MST represents the atmospheric water vapor tendency due to precipitation, so that condensation is negative. The full field and anomalies from the mean are shown to demonstrate the interannual variability of the terms. Some of the largest changes in the precipitation tendency (MST, Figure 7 e and f) occur within the boundary layer (between the surface and 800 hPa), where condensation is being substantially reduced. While the analysis increment is adding some water back in the PBL (Figure 7 c and d). However, the analysis is adding more water in the middle troposphere (between 800 and 500 hPa), where it is then is increasing the divergence. The turbulent tendency reflects the reduction in surface evaporation. Since the only source of water for land evaporation is precipitation, the changes in evaporation are following that of the precipitation. Figure 8 shows a comparison of the water budget tendency profiles before and after 2001. The peak reduction of water in the column due to precipitation processes (MST) has a maximum at the top of the boundary layer. Turbulent mixing provides a large source of water for precipitation in the upper portion of the boundary layer, and is significantly reduced after 2001. While the analysis increment is positive (adding water due to the observational analysis), the change after 2001 is primarily above 800 hPa. The question remains, if the analysis is adding water into the lower atmosphere and boundary layer, then why does precipitation decrease?

In separating the analysis increment into time series for each of the diurnal analysis times (Figure 9), we find distinct interannual variations for each analysis time but especially different between analyses with radiosonde observations (00Z and 12Z) and those without radiosondes (06Z and 18Z). For example, at 06Z analysis tendencies for water vapor were quite small (and uniformly negative throughout the column) until early 2001, when they become abruptly large positive between 800 and 500 hPa. This shift is toward strongly positive increments at 700hPa, mostly above the boundary layer. A similar shift occurs in the 18Z analysis time, though it becomes strongest in early 2003. In order to objectively identify a time of this transition, we use the change point test developed by Lund and Reeves (2002) on the 700 hPa water vapor increments. The result indicates a statistically significant change point in April 2001 at 06Z and 18Z (though the 18Z maximum in the change point test is found in Feb 2003). Conversely, 00Z and 12Z do not yield any statistically significant change points. The presence of radiosondes may provide a stabilizing factor, or at least, any changes in the radiosonde observing system are not enough to make a significant shift in the time series. For the whole reanalysis period, the 12Z (early morning) analysis is adding water into the lowest layers of the troposphere. The analysis increment at 18Z is removing water from within the boundary layer during the daytime (Figure 6) when MERRA produces most precipitation in this region. Figure 10 compares the mean profiles of ANA and MFD before and after 2001. The 06Z and 18Z change in ANA is pronounced. What were once small increments have increased magnitude substantially, and the 06Z and 18Z MFD changes follow the ANA vertical distribution. It seems likely then that the ANA reduction in daytime (18Z) boundary layer moisture is slowing the production of precipitation, which in turn is the limit of land evaporation. This is contrary to the 12Z (morning) analysis increments. Before 2001, the 12Z increments were tending to add moisture to the lowest layers, and after 2001, this tendency doubled. The 00Z and 12Z analyses include the radiosonde observations, which in turn, also constrain the analysis of satellite radiances, through variational bias correction (Dee and Uppala 2009). In order to evaluate this further, information on the observations is needed.

c. Observing System Evaluation

Observations are the critical component of a reanalysis system, as the system reverts to model simulation (along with its climatological biases) when observations are lacking. Over the US, there are substantial numbers of observations for most of the modern satellite period. The abundance of observations over the US generally implies that the reanalysis climatology and climate variability should be of high quality. Likewise, dynamical terms, such as MFD, should be more reliable than those derived from model physics, such as E-P (Trenberth et al. 2011). Yet, a shift occurs in the MFD climatology in both MERRA and ERA-I (Figure 2) that, thus far, appear related to the observational analysis. In this section, we use the MERRA Gridded Innovations and Observations (GIO) data to investigate the observing system.

Figure 11 shows the spatial and temporal data count of radiosonde derived specific humidity in MERRA. The data provided in GIO are only those that have been assimilated (data rejected from assimilation are not included). In the central US region we are investigating, the radiosonde observations tend to be grouped in the southern third, with another group of stations near the northern third. Over time, the spatial distribution of the stations does not noticeably change (not shown). Of course, when looking at the vertical distribution, mandatory levels have substantially more observations than significant levels. The temporal variability of the radiosonde data contains many changes, some large, some more subtle. It is difficult to account for every fluctuation in the time series, though the introduction of 925 hPa as a mandatory level appears around 1992. There are numerous changes in radiosonde instrumentation that may affect the climate record (e.g. Elliott et al. 2002). In MERRA, certain shifts and biases have been corrected (Haimberger 2007; Rienecker et al. 2011), though these are for temperature measurements.

The observed water vapor profiles show some year-to-year variability, but there is no indication of a change in the water vapor (Figure 12 a and b) that might be related to shift in the water budget after 2000 (Figure 4). The analysis of RAOB water vapor differs between 00Z and 12Z, where the 12Z forecast is steadily dry in the lower troposphere throughout the period, while the 00Z forecast shows fluctuations especially nearer the surface (Figure 12 c and d). There is a distinct separation of positive and negative forecast bias between the upper and lower troposphere. The level of this separation seems to decrease in altitude for 00Z and increase for 12Z after 2000. It is clear that these variations are not consistent with the sudden change in the total increment at 06Z and 18Z (Figure 9 and Figure 10). The radiosondes provide some stability (regarding analyzed data) for the 12Z and 00Z analysis. However, it is of note that the RMS of the radiosonde forecast departures decrease over the reanalysis period, all the way through to the most recent years (Figure 12 e and f). The mandatory radiosonde levels also show lower RMS of the forecast departures than the significant levels.

The comparison of the ANA and MFD tendencies shows that, for this region, they are correlated well at large space and time scales (e.g. Figure 2 and Figure 3). While the ANA term is generally related to the water vapor analysis, MFD would be a function of both moisture and wind. The previous discussion suggests that radiosonde water vapor assimilation is not likely involved with the shift in water vapor increments. Conventional wind observations are somewhat more complicated, considering that wind observations are available in all the analysis cycles. There tend to be some increases in the aircraft wind observations after 2000, when Velocity Azimuth Display (VAD) wind profiles start to be assimilated. Some time was taken to evaluate the wind observing system as was presented with the radiosonde water vapor observations. While there are changes to the observing systems around 2000 due to the increase in number of observations (Figure 13), it is not clear that these would lead to a systematic change in the moisture flux divergence. The wind increment change would need to be arranged as to increase divergence. Such a persistent arrangement seems unlikely to occur and maintain, and was not obvious in evaluation of the background forecast and analysis winds. However, wind observations do serve to demonstrate the complexities of the observing system, and also the difficulty in determining the physical response of the system to analyzed observations.

d. *Satellite Observation Sensitivity*

As diverse as the conventional observations are (including satellite data retrievals of physical quantities), the satellite radiances that are assimilated add complexity and data volume to the input data records. In this first version of GIO, we have elected to simplify the satellite data by not producing grids every 6 hours, as with conventional data, but provide monthly and monthly diurnal cycle (4 analysis times per month). These include the average brightness temperatures and forecast departures for each month including the data count for each grid point. Consider that each instrument has multiple channels and spatial distribution at each analysis time. Multiple instruments may exist at any given time and any given region, though whether their orbits allow for observations to coexist and be assimilated in a given analysis cycle is not necessarily easily diagnosed. We first look at the available satellite observations in the region of interest to ascertain any obvious changes in the satellite observing system that may lead to changes in the analysis increment and water budget.

Rienecker et al. (2011) presents a table of satellite systems assimilated in MERRA. Notably, NOAA15’s introduction of the AMSUA instrument in late-1998 led to significant shift in the global water cycle, though it appeared most influential over certain oceanic regions and land regions water cycle variations did not stand out (Robertson et al. 2011; Bosilovich et al. 2011). However, as discussed previously, the change point detection applied to the central US shows spikes for 06Z and 18Z at April 2001, not long after the introduction of the first AMSUA (Sept. 1998).

As an example, Figure 14 shows the data count for AMSUA channel 2 (a window channel) assimilated in MERRA for the central US region. When NOAA15 AMSUA is introduced (AM orbit), only a very small number of observations occur in the central US at 18Z and none in the 06Z analysis. However when NOAA16's PM orbit is introduced (Nov 2000), coverage is primarily in 06Z and 18Z in the central US (crossing time drift affects the NOAA16 data counts over time). The assimilated AMSUA channel 2 data count also has a seasonal cycle peaking in the warm season (all window channels exhibit a similar seasonality, not shown). So that, any seasonally varying NOAA16 data (e.g. AMSUA, AMSUB and HIRS3) assimilation first appears in 06Z analysis in the 2001 warm season. Aqua-AMSUA is assimilated beginning in the end of 2002, so that 2003 is the first warm season where that instrument is used. Its 06Z and 18Z counts indicate it is also of significance for water vapor in the seasonal cycle.

Satellite systems document the quality of remotely sensed data and when channels are disabled, but this information is not centrally available relative to a reanalysis for all available instruments and channels. Furthermore, one aspect of the satellite observing system not easily documented is the regional distribution of data accepted and assimilated in a reanalysis. A strength of GIO data is that this information is easily accessible, and flexible enough for consideration in most projects. As an example, we use GIO to characterize the satellite observations assimilated in MERRA, over the central US in the late 1990s and 2000s when this unphysical long-term moisture flux divergence occurs.

By the end of 2007, both NOAA16 and Aqua AMSUA channel 4 experience problems and are turned off (all of NOAA16 AMSUA is turned off then). However, the Aqua-AMSUA window and other channels continue to be assimilated after channel 4 is excluded. Starting in 2008, the number of Aqua AMSUA window channel observations being assimilated increases in the Central US region,. In addition, NOAA17 only provided data for a limited period of 2005-2006, while NOAA18 started providing data in 2006. Considering the data counts suggests that the NOAA16 overflight of the central US region could affect the 06Z and 18Z analyses, while Aqua in 2003 appears concurrent with significant variations in the 18Z analysis (comparing Figure 14 with Figure 9). It is also worthwhile to note that the 18Z analysis window includes the local solar noon time and associated surface heating.

Figure 15 shows the forecast departures (observation minus forecast, OmF) at each analysis cycle for each platform's AMSUA Channel 5 radiance (a channel sensitive to lower troposphere temperature). At 06Z, the forecast departures are positive, although, each analysis cycle seems to have its own temporal variations. The NOAA15 AMSUA channel 5 forecast departures exhibit a gradual trend at 00Z, but at 12Z they jump near 2008, along with the other available AMSUA instruments. Channel 5 data counts (not shown) generally follow the relative pattern of channel 2 data counts (Figure 14). It is worthwhile noting that the NOAA15 and NOAA18 Channel 4 forecast departures and analysis increments rise sharply following the loss of NOAA16 AMSUA and Aqua AMSUA Channel 4 (not shown). AMSUA channel 4 is sensitive to the water burden in the lower troposphere, and the change in available data affects the analysis of other channels.

As MERRA was evolving and producing longer time series, it was not immediately obvious that AMSUA should be as influential on the US regional water cycle, as this evaluation shows. Early sensitivity tests showed strong signals over the southern oceans and warm pool regions than over land (Bosilovich et al. 2011). However, we now see the impact of observing system variations, especially from remote sensing platforms over land, was obscured by the variations in the diurnal cycle and the presence of radiosonde observations. Even so, aboard the

NOAA satellites are also HIRS3 and AMSUB instruments, each with channels sensitive to the water vapor (though their impact on global and hemispheric forecast error tend to be less than AMSUA, as discussed by Gelaro and Zhu 2009). Likewise, AMSUB and HIRS3 instruments occasionally have different availability in the historical record due to instrument or channel failures. AIRS is another consideration, with more than 150 channels assimilated in MERRA, it holds the largest volume of data used in MERRA, though the impact of AIRS on global forecast error is also less than AMSUA (Gelaro and Zhu 2009).

In order to define which instrument(s) contributes to the water vapor analysis increment profile that causes the MFD signal in the central US, we performed a series of data withholding experiments, individually removing AMSUB, HIRS3, AMSUA and AIRS. Since the signal in the analysis increments peaks in summer and also occurs with regularity between 2001-2006, we performed the sensitivity tests for one month, July 2005 on each instrument. Figure 16 shows the control analysis increment for July 2005, and the contribution of each instrument to that increment, as determined by individually withholding that instrument. The impact on the anomalous water vapor increments in the central US is not related to HIRS3 or AMSUB assimilation. The small effect of these channels may be in line with the assimilation of previous instruments, like HIRS2, considering the 06Z and 18Z increments early in the reanalysis period shown in Figure 9.

Withholding AMSUA largely removed the 06Z drying increments below 850 hPa and a fraction of increments above 700 hPa. The assimilation of AIRS accounts for the strong positive water vapor increments centered at 700 hPa in the 06Z analysis. In the 18Z analysis, AUMSUA is causing the large positive increments at 700 hPa with some contribution from AIRS, though AIRS contribution to drying above 500 hPa is also apparent. Subsequent tests were designed to identify the AMSUA channels leading to the strong water vapor increments. ASMUA window channels (1, 2, 3, and 15) are the primary cause of the boundary layer drying increments (Figure 17). In the 18Z analysis, the window channels are only partly contributing to the peak source of water at 700 hPa. The other part (from 700 hPa to the surface) comes from channel 5, which is sensitive to the atmospheric temperature. Channel 4, which is sensitive to the water vapor, plays a much smaller role on the water vapor increments, but does add water at 700 hPa and remove water in the PBL. In subsequent NASA reanalyses, AMSUA window channels will not be included in the assimilation for impacts much more global than identified here (Rienecker et al. 2011). At this point, we have not tried to isolate the AIRS channel contributions. The influence and appropriateness of AIRS and AMSUA Channel 5 on the continental US water vapor increments will require further study.

4. Summary and conclusions

Reanalyses continue to be developed and improved over time, and the research community demands more quality and detail in global and regional processes. However, the crucial underlying observing system is a complex collection of diverse variables, each with incomplete spatial and temporal coverage. Ideally, we would like to be able to assess inconsistencies in the resulting reanalysis and identify physical improvements to the system, such as the suggestion to incorporate irrigation as a source of water in the Central US to improve the water cycle there (as suggested by Trenberth et al. 2011 in regards to Figure 1). In this study, we investigate a deficiency in the physical fields of the regional water budget of the Central United States, then use the closed regional water budget, three dimensional water vapor analysis increments and the assimilated observations to evaluate the reanalysis data.

Vertically integrated water vapor increments are related to an anomalous MFD feature presented in Figure 1, which starts in the early 2000s, but before that had more realistic features (in other words, the negative divergence implies more precipitation than evaporation). The vertically integrated MFD and increments only revealed part of the problem, as there was a distinct positive increment, yet precipitation decreased while the divergence increased. This is explained by looking at the vertical profiles of MFD and the analysis increment, but only after the diurnal variations of the 4 analysis cycles are considered individually. The water vapor increments change dramatically around March 2001, but especially in the 06Z and 18Z analysis cycles, where water vapor was being added above the boundary layer and the analysis increments were taking away water in the lowest layer. This time is also collocated with the first warm season to include NOAA16 data assimilation, including AMSUA, AMSUB and HIRS3. NOAA16's orbit at launch covered the Central US during the 06Z and 18Z analysis cycles initially (crossing time drift affects that over a period of years). However, the Aqua AMSUA and AIRS instruments began providing data at the end of 2002 and also contributed to the 06Z and 18Z analysis cycles in the central US. Observing system experiments narrowed the source of the changing analysis increments (and hence MFD) to the assimilation of AMSUA window channels and channel 5, but also AIRS.

The GIO data provide a fundamental part of evaluating the observing system and its variations in time over this region. The gridding permits quantitative evaluation that can be performed across all the assimilated observations, from radiosonde to radiance. While these data are produced for all reanalyses, they are generally in formats that require additional time and effort to use, and may also be more difficult to gain access. The gridded observations guided sensitivity tests to isolate the systems that affect the water vapor increments in the Central US.

In subsequent work, we hope to evaluate the forecast departure and analysis increments of each observing type, along with more advanced diagnostics of the analysis (e.g. Desroziers et al. 2005). Likewise, we are revisiting the formulation of the gridding process to provide as much information about the analysis. For example, this initial form of GIO did not include the variational bias corrections used for radiance assimilation (Dee and Uppala 2009), and that could provide additional information to evaluate the various observing systems and channels.

Acknowledgments

This work was supported by NASA's Energy and Water Cycle Studies program (NEWS) and also the NASA's Modeling and Analysis Program (MAP). King-Sheng Tai's effort in producing the sensitivity studies is greatly appreciated. We also thank Christopher Redder for his initial efforts in developing the GIO data files.

5. Appendix: Acronyms

AIRS Atmospheric Infrared Sounder
AM Here, referring to a satellite's morning sun-synchronous orbit
AmF Analysis minus Forecast
AMSU Advanced Microwave Sounding Unit (sometimes with versions A and B)
ANA Indicates the analysis increment term of the reanalysis water vapor budget
ATOVS Advanced TIROS Operational Vertical Sounder
CMAP NOAA Climate Prediction Center (CPC) Merged Analysis of Precipitation
CPCU NOAA Climate Prediction Center (CPC) Unified Precipitation Analysis
ECMWF European Centre for Medium Range Weather Forecasts
ERA-I ECWMF Interim Reanalysis
GEOS-5 Goddard Earth Observing System (Version 5)
GIO Gridded Innovations and Observations
GMAO Global Modeling and Assimilation Office
GPCP Global Precipitation Climatology Project
HIRS High-resolution Infrared Radiation Sounder
IAU Incremental Analysis Update
MERRA Modern Era Retrospective-analysis for Research and Applications
MFD Moisture Flux Divergence

MSU Microwave Sounding Unit
NASA National Aeronautics and Space Administration
NOAA National Oceanic and Atmospheric Administration
OmA Observations minus Analysis
OmF Observation minus Forecast
PBL Planetary Boundary Layer
PM Here, referring to a satellite's sun-synchronous afternoon orbit
RAOB Radiosonde Observation
SSM/I Special Sensor Microwave Imager
SSU Stratospheric Sounding Unit
TIROS Television Infrared Observation Satellite

6. References

Bloom, S., L. Takacs, A. da Silva, and D. Ledvina, 1996: Data assimilation using incremental analysis updates. *Mon. Wea. Rev.*, **124**, 1256-1271.

Bosilovich, M.G., F. R. Robertson, and J. Chen, 2011: Global energy and water budgets in MERRA. *J. Climate*, **24**, 5721–5739. doi: 10.1175/2011JCLI4175.1

Dee, D. P., and S. Uppala, 2009: Variational bias correction of satellite radiance data in the ERA-Interim reanalysis. *Q. J. R. Meteorol. Soc.*, **135**, 1830–1841. doi: 10.1002/qj.493

Dee, D. P., and co-authors, 2011: The ERA-Interim reanalysis: configuration and performance of the data assimilation system. *Q. J. R. Meteorol. Soc.*, **137**, 553–597. DOI:10.1002/qj.828

Desroziers, G., L. Berre, B. Chapnik, and P. Poli, 2005: Diagnosis of observation, background and analysis-error statistics in observation space. *Q. J. R. Meteorol. Soc.*, **131**, 3385–3396.

Elliott, W. P., R. J. Ross, and W. H. Blackmore, 2002: Recent changes in NWS upper-air observations with emphasis on changes from VIZ to Vaisala radiosondes. *Bull. Amer. Meteor. Soc.*, **83**, 1003–1017. doi: http://dx.doi.org/10.1175/1520-0477(2002)083<1003:RCINUA>2.3.CO;2

Gelaro, R., and Y. Zhu, 2009: Examination of observation impacts derived from observing system experiments (OSEs) and adjoint models. *Tellus*, **61A**, 179–193.

Haimberger, L., 2007: Homogenization of radiosonde temperature time series using innovation statistics. *J. Climate*, **20**, 1377–1403. doi: http://dx.doi.org/10.1175/JCLI4050.1

Kanamaru, H., and G. D. Salvucci, 2003: Adjustments for wind sampling errors in an estimate of the atmospheric water budget of the Mississippi River Basin. *J. Hydrometeor*, **4**, 518–529.

Lund, R., and J. Reeves, 2002: Detection of undocumented changepoints: A revision of the two-phase regression model. *J. Climate*, **15**, 2547–2554. doi: http://dx.doi.org/10.1175/1520-0442(2002)015<2547:DOUCAR>2.0.CO;2

Ozdogan, M., and G. Gutman, 2008: A new methodology to map irrigated areas using multi-temporal MODIS and ancillary data: An application example in the continental US. *Rem. Sens. Env.*, **112**, 3520-3537.

Ozdogan, M., M. Rodell, H. Kato Beaudoing, and D. L. Toll, 2010: Simulating the effects of irrigation over the United States in a land surface model based on satellite-derived agricultural data. *J. Hydromet.*, **11**, 171–184.

Reichle, R., R. D. Koster, G. J. M. De Lannoy, B. A. Forman, Q. Liu, S. P. P. Mahanama, and A. Toure, 2011: Assessment and enhancement of MERRA land surface hydrology estimates. *J. Climate*, **24**, 6322–6338. doi: http://dx.doi.org/10.1175/JCLI-D-10-05033.1

Rienecker, M. R., and co-authors, 2011: MERRA - NASA's Modern-Era Retrospective Analysis for Research and Applications. *J. Climate*, **24**, 3624–3648.

Robertson, F. R., M. G. Bosilovich, J. Chen, and T. L. Miller, 2011: The effect of satellite observing system changes on MERRA water and energy fluxes. *J. Climate*, **24**, 5197–5217.

Roads, J. O., M. Kanamitsu, and R. Stewart, 2002: CSE water and energy budgets in the NCEP-DOE reanalysis II. *J. Hydromet.*, **3**, 227-248.

Trenberth, K. E., J. T. Fasullo, and J. Mackaro, 2011: Atmospheric moisture transports from ocean to land and global energy flows in reanalyses. *J. Climate*, **24**, 4907–4924. doi: http://dx.doi.org/10.1175/2011JCLI4171.1

Yarosh, E. S., C. F. Ropelewski, and E. H. Berbery, 1999: Biases of the observed atmospheric water budgets over the central United States. *J. Geophys. Res.*, **104**, 19349–19360. doi: 10.1029/1999JD900322.

7. Tables

Table 1. Time correction coefficiences of annual mean water budget terms over the central United State from 1979 to 2012.

	P	***E***	***E-P***	***MFD***	***ANA***
P	**1.00**				
E	**0.92**	**1.00**			
E-P	**-0.54**	**-0.18**	**1.00**		
MFD	**-0.79**	**-0.69**	**0.51**	**1.00**	
ANA	**-0.66**	**-0.71**	**0.15**	**0.93**	**1.00**

8. List of Figures

Figure 1 Mean vertically integrated moisture flux divergence (mm day^{-1}) from MERRA (left) and ERA-I (Dee et al. 2011; right) reanalysis for 2001-2012 (top) and 1979-2000 (bottom). The red box in a) indicates the central United States region (101^{o}-94^{o} W, 34^{o}-46^{o} N) that has positive moisture flux divergence for 2001-2012.

Figure 2 Time series of annual mean vertically integrated moisture flux divergence (mm day^{-1}) over the central United States (red box in Figure 1a) from MERRA and ERA-I reanalyses.

Figure 3 MERRA annual mean a) evaporation, b) vertically integrated moisture flux divergence, c) precipitation, d) vertically integrated analysis increment, and e) evaporation minus precipitation (E-P) for the period 2001-2012. All units are in mm day^{-1}.

Figure 4 Time series of annual mean vertically integrated moisture budget (mm day^{-1}) over the central United States from MERRA and MERRA-Land (MLD).

Figure 5 Annual cycle of vertically integrated moisture budget (mm day^{-1}) over the central United States for period 1979-2000 (dot lines) and 2001-2012 (solid lines).

Figure 6 Diurnal cycle of vertically integrated moisture budget (mm day^{-1}) over the central United States for period 1979-2000 (dot lines) and 2001-2012 (solid lines).

Figure 7 Time-height cross section of annual mean water vapor tendency terms (left) over the central United States and their anomalies (right) from 1979-2012 climate mean. All units are in g kg^{-1} day^{-1}. Here, MST represents the precipitation processes (including all phases of condensation and rain evaporation) and TRB represents turbulence tendencies (vertically integrates to surface evaporation).

Figure 8 Vertical profiles of water vapor tendency terms (g kg^{-1} day^{-1}) over the central United States for period 1979-2000 (dot lines) and 2001-2012 (solid lines).

Figure 9 Time-height cross section of annual mean water analysis increment (g kg^{-1} day^{-1}) at a) 00Z, b) 06Z, c) 12Z, and d) 18Z over the central United States.

Figure 10 Vertical profiles of water vapor tendency ANA and MFD terms at a) 00Z, b) 06Z, c) 12Z, and d) 18Z over the central United States for period 1979-2000 (dot lines) and 2001-2012 (solid lines). All units are in g kg^{-1} day^{-1}.

Figure 11 Annual mean number of observations (in thousands) for (a) RAOB stations in the United States from 1000 to 300 hPa (21 constant pressure levels) (b) time-height cross section over the Central United States box.

Figure 12 Annual mean water vapor mixing ratio observations (top), analysis departure (middle), and root mean square error of forecast departure (bottom) from RAOB over the central United States at 00Z (left) and 12Z (right). All units are in g kg^{-1}.

Figure 13 The annual number of meridional wind observations (in thousands) over the central United States for wind from a) Radiosonde, b) LIDAR profiler, c) Aircraft, d) VAD. A technical coding error lead for the MERRA input data lead to the wind profiler gap during 2006-2007.

Figure 14 Monthly data count over the central US region for all platforms, NOAA15 (a), NOAA16 (b), NOAA18 (c), and Aqua (d), of AMSUA window channel 2, where each line indicates an analysis time. Lines may overlap, especially if no observations were present. These counts reflect the observations that were assimilated, and not the actual number of observations that may be available. Also, data thinning affects the number reported here.

Figure 15 Monthly forecast departures (O-F) for AMSUA channel 5 brightness temperatures (K) over the central US region, separated by analysis time (a-d).

Figure 16 Contribution of selected instruments (AMSUA, AMSUB, HIRS3, and AIRS) to monthly mean ANA tendency (g kg^{-1} day^{-1}) at (a) 06Z and (b) 18Z over the central US region in July 2005. Control experiment (CONTROL) has all observations as MERRA. The contribution of each instrument is the difference between the control experiment and each instrument's data withholding experiment. SUM is the summation of AMSUA, AMSUB, HIRS3, and AIRS.

Figure 17 Contribution of AMSUA and its selected channels (window channels, channel 4 and channel 5) to monthly mean ANA tendency (g kg^{-1} day^{-1}) at (a) 06Z and (b) 18Z over the central US region in July 2005. Window channel includes channel 1, 2, 3 and 15. The contribution of each channel is the difference between the control experiment and each channel's data withholding experiment. SUM is the summation of window channels, channel 4, and channel 5.

9. Figures

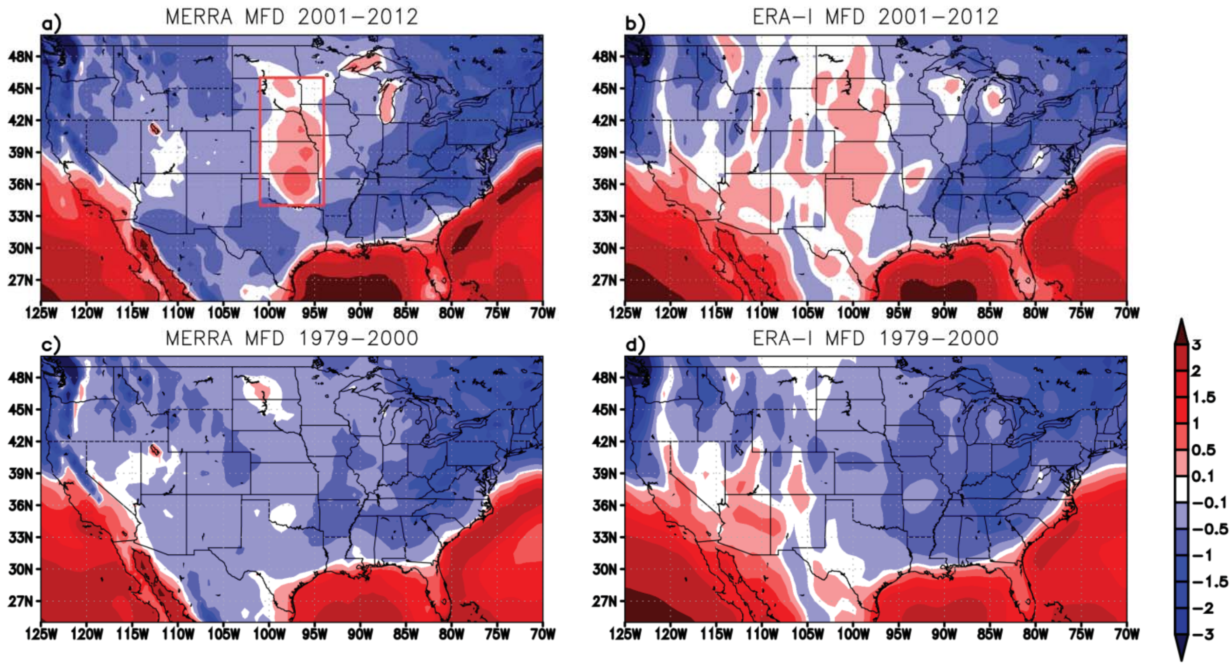

Figure 1 Mean vertically integrated moisture flux divergence (mm day^{-1}) from MERRA (left) and ERA-I (Dee et al. 2011; right) reanalysis for 2001-2012 (top) and 1979-2000 (bottom). The red box in a) indicates the central United States region (101^{o}-94^{o} W, 34^{o}-46^{o} N) that has positive moisture flux divergence for 2001-2012.

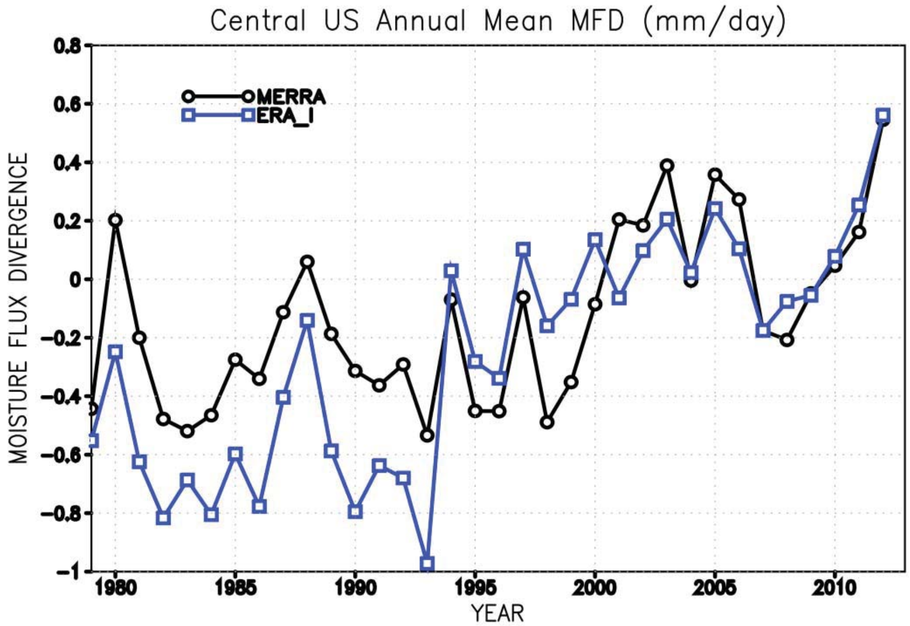

Figure 2 Time series of annual mean vertically integrated moisture flux divergence (mm day^{-1}) over the central United States (red box in Figure 1a) from MERRA and ERA-I reanalyses.

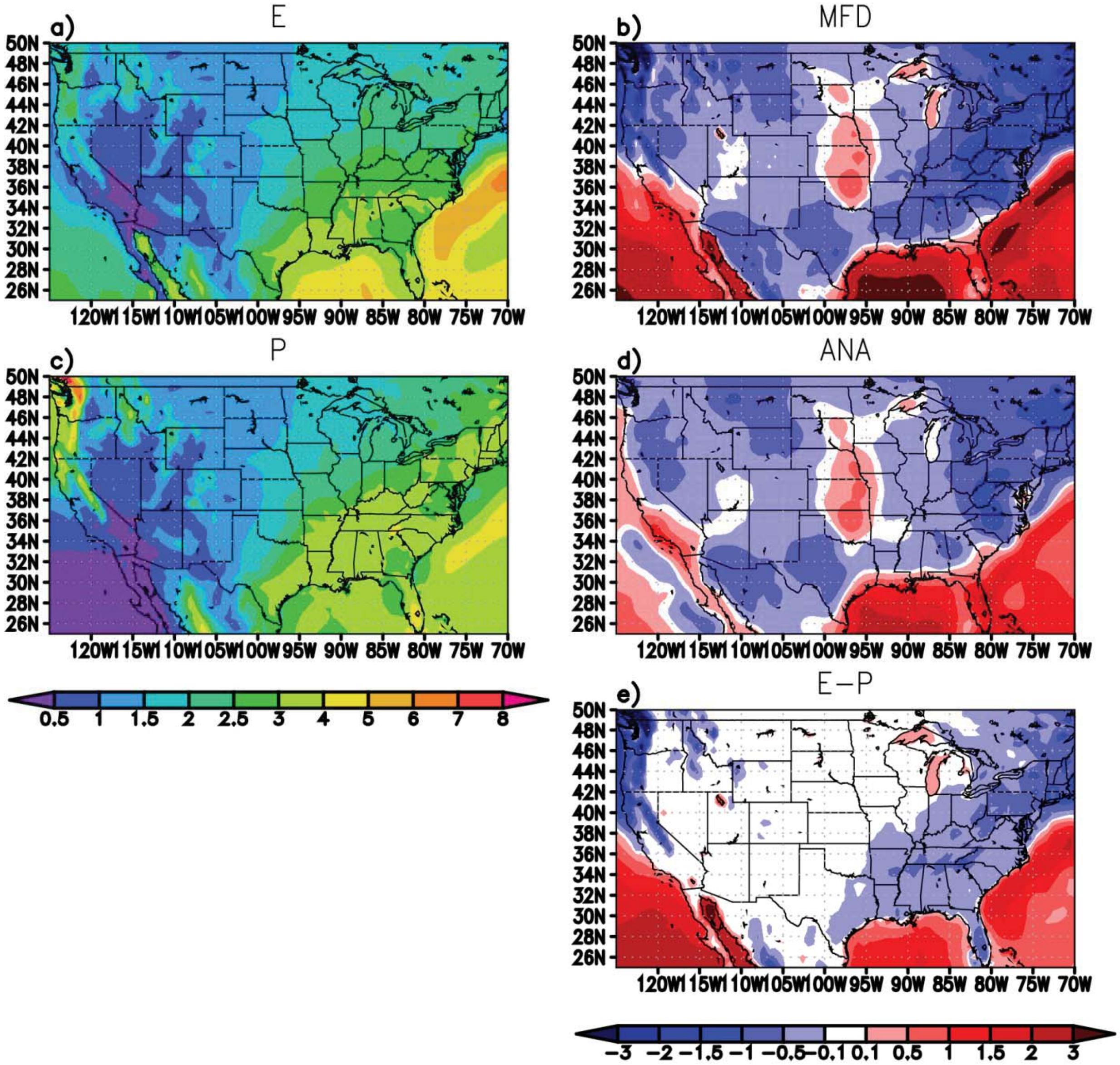

Figure 3 MERRA annual mean a) evaporation, b) vertically integrated moisture flux divergence, c) precipitation, d) vertically integrated analysis increment, and e) evaporation minus precipitation (E-P) for the period 2001-2012. All units are in mm day^{-1}.

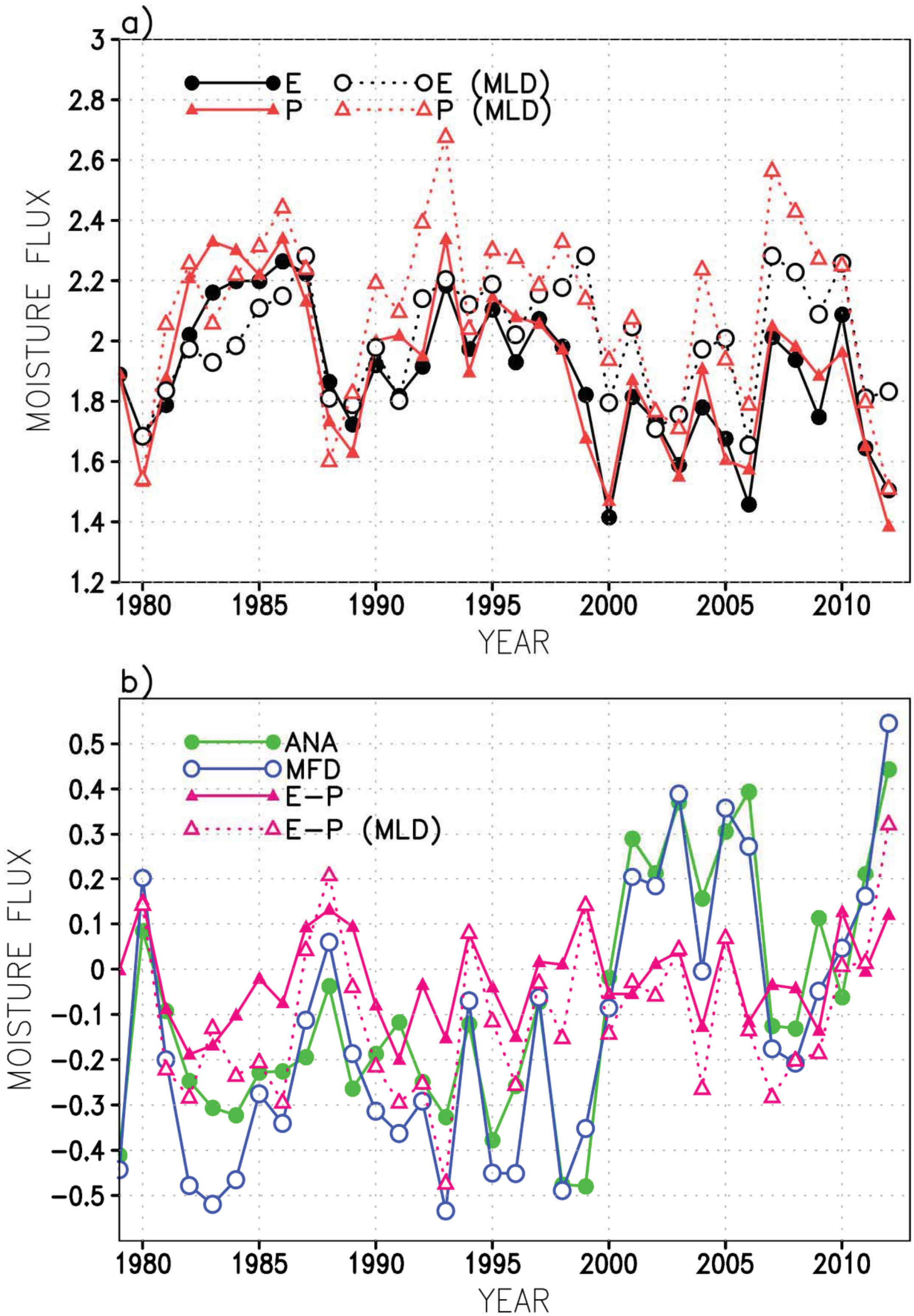

Figure 4 Time series of annual mean vertically integrated moisture budget (mm day^{-1}) over the central United States from MERRA and MERRA-Land (MLD).

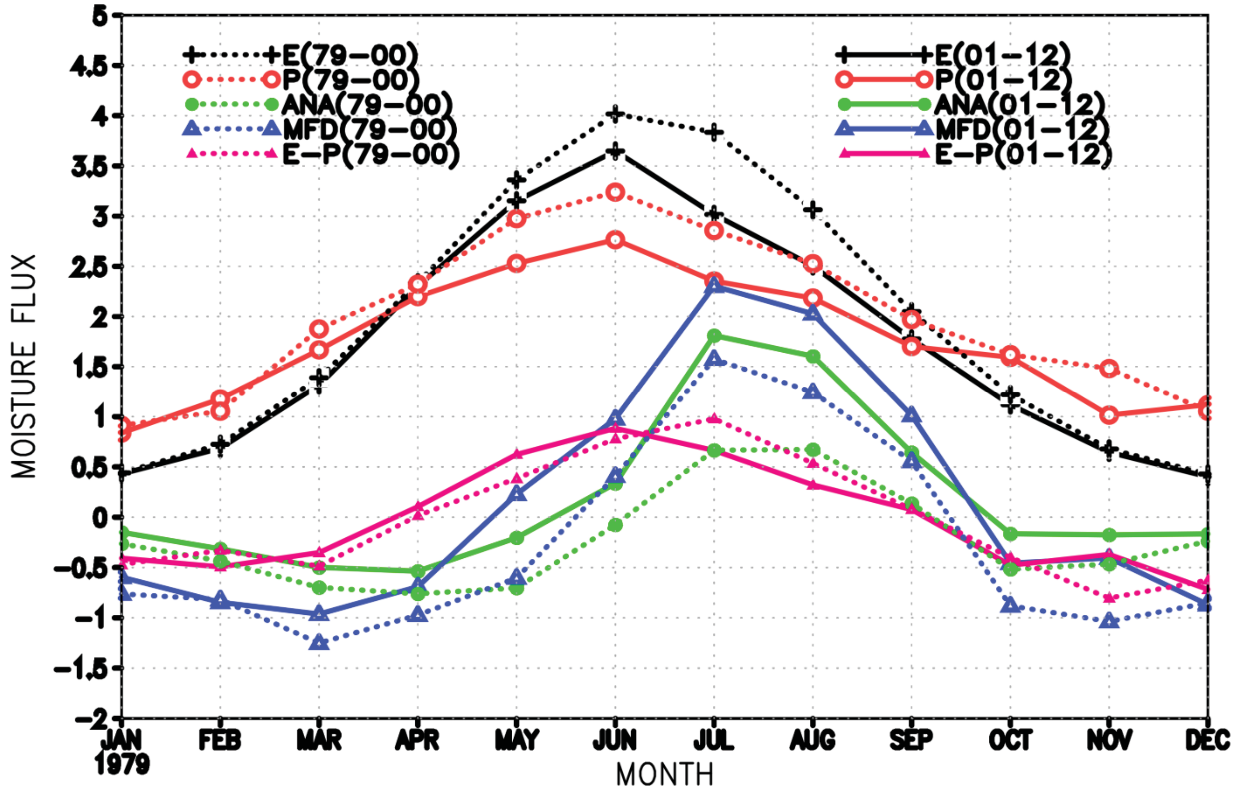

Figure 5 Annual cycle of vertically integrated moisture budget (mm day^{-1}) over the central United States for period 1979-2000 (dot lines) and 2001-2012 (solid lines).

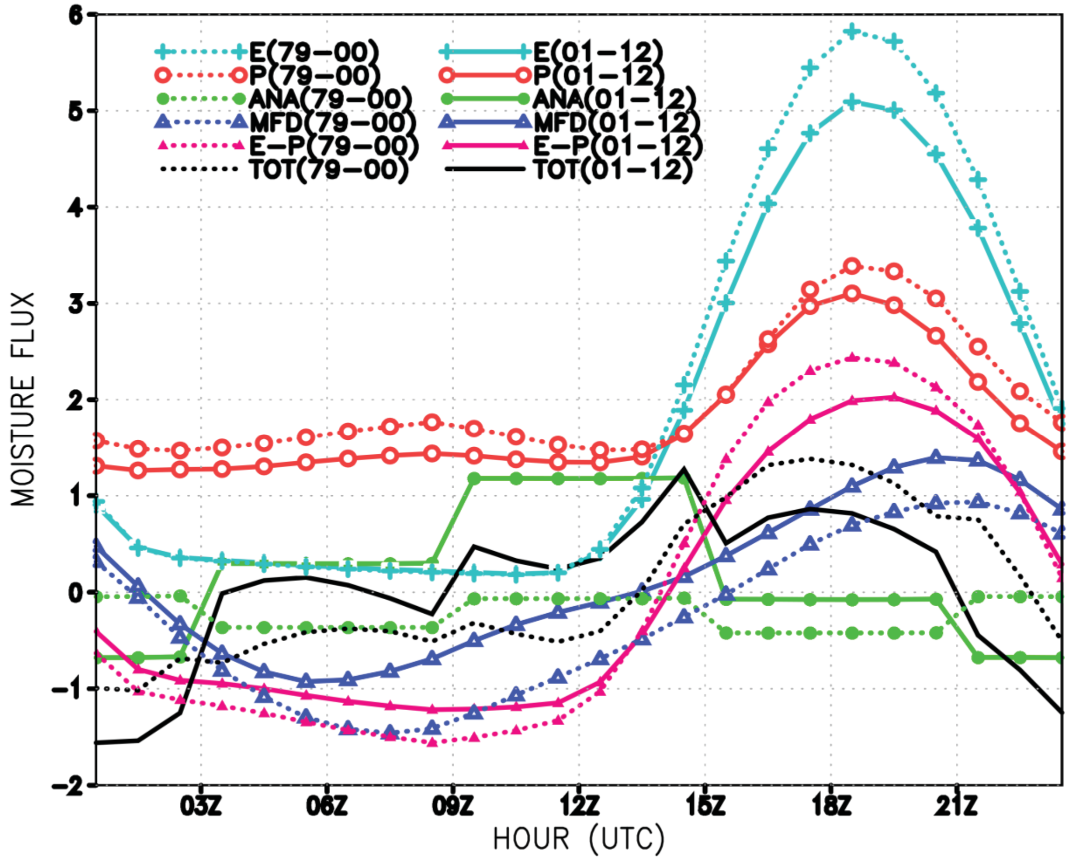

Figure 6 Diurnal cycle of vertically integrated moisture budget (mm day^{-1}) over the central United States for period 1979-2000 (dot lines) and 2001-2012 (solid lines).

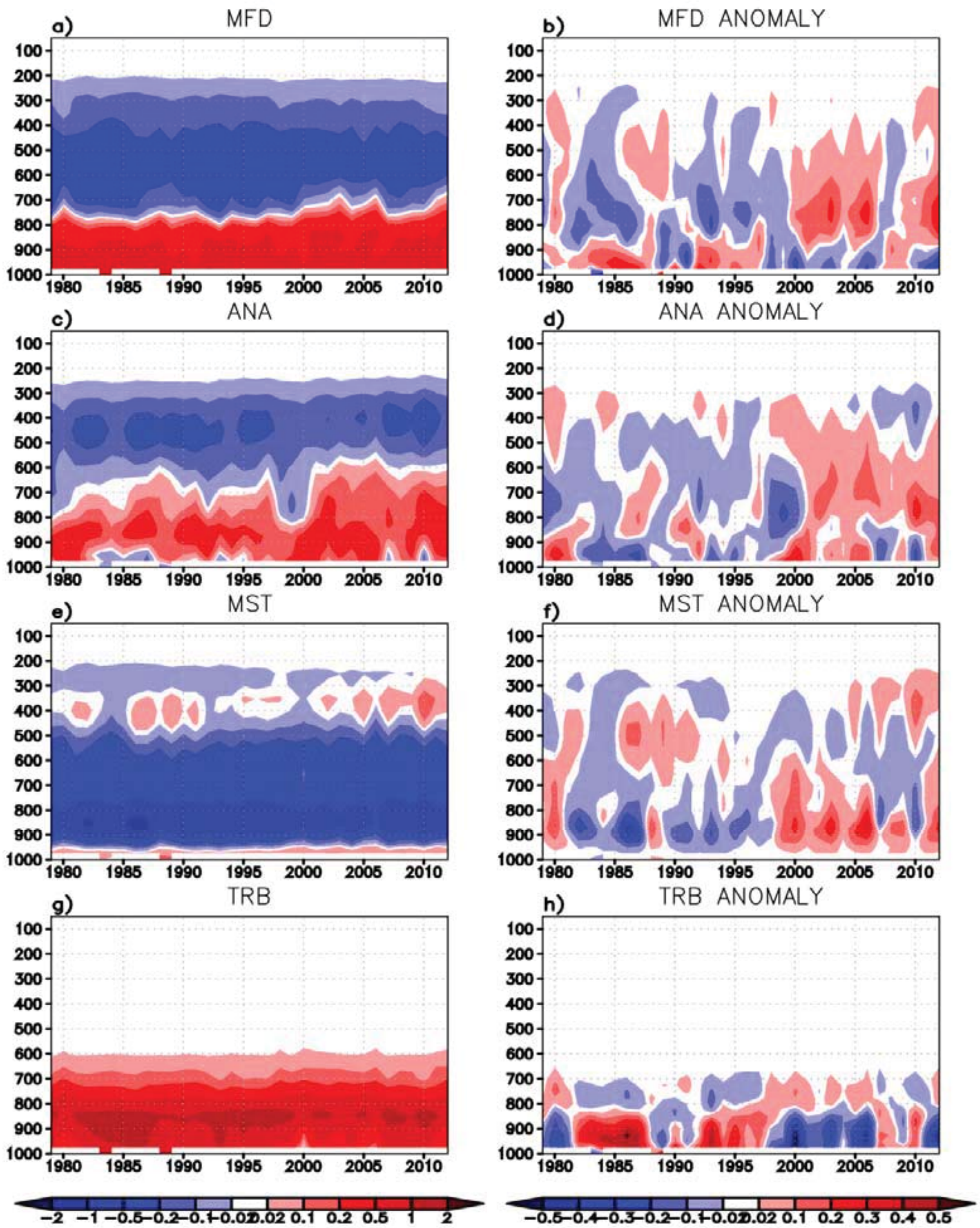

Figure 7 Time-height cross section of annual mean water vapor tendency terms (left) over the central United States and their anomalies (right) from 1979-2012 climate mean. All units are in g kg^{-1} day^{-1}. Here, MST represents the precipitation processes (including all phases of condensation and rain evaporation) and TRB represents turbulence tendencies (vertically integrates to surface evaporation).

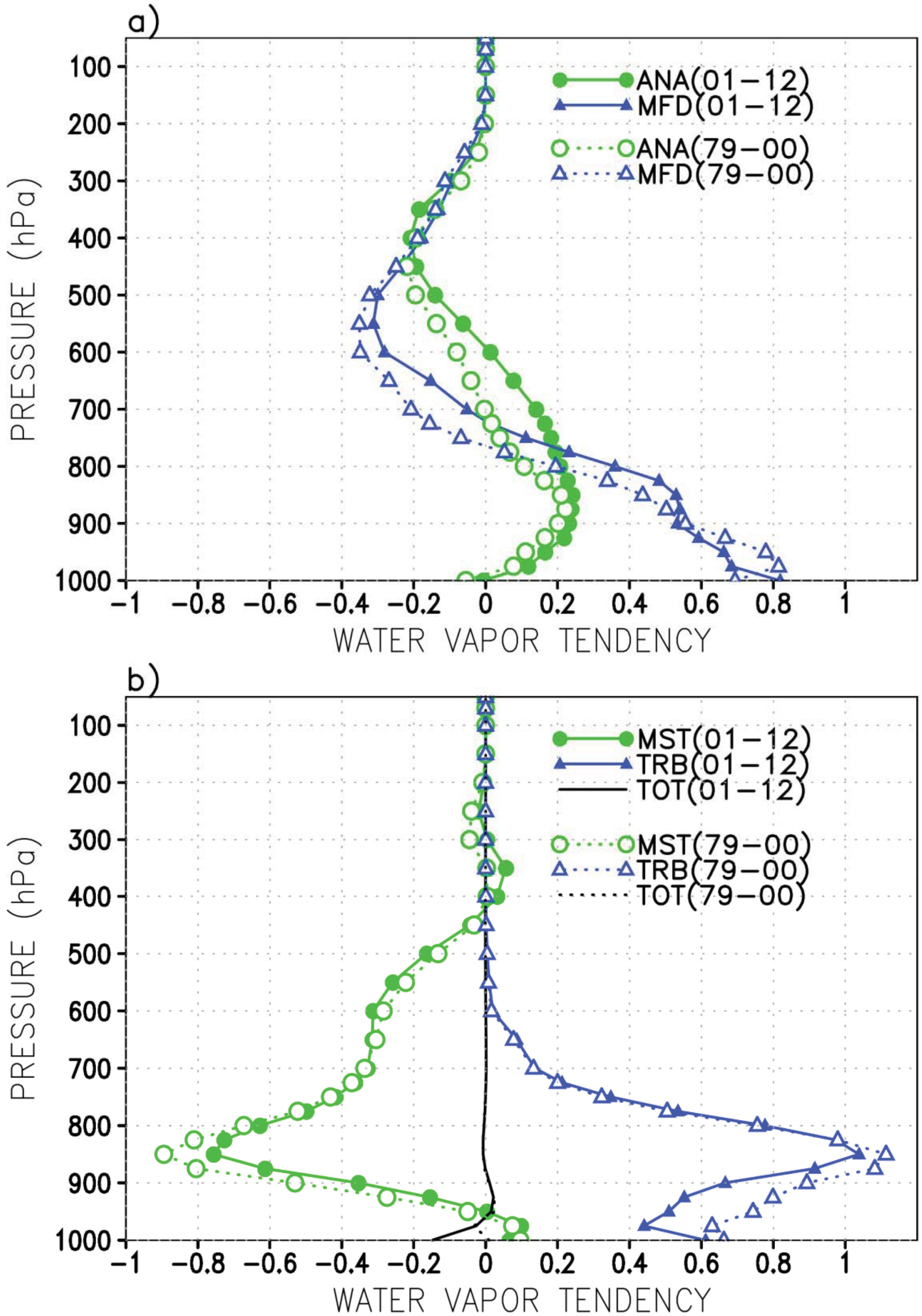

Figure 8 Vertical profiles of water vapor tendency terms (g kg^{-1} day^{-1}) over the central United States for period 1979-2000 (dot lines) and 2001-2012 (solid lines).

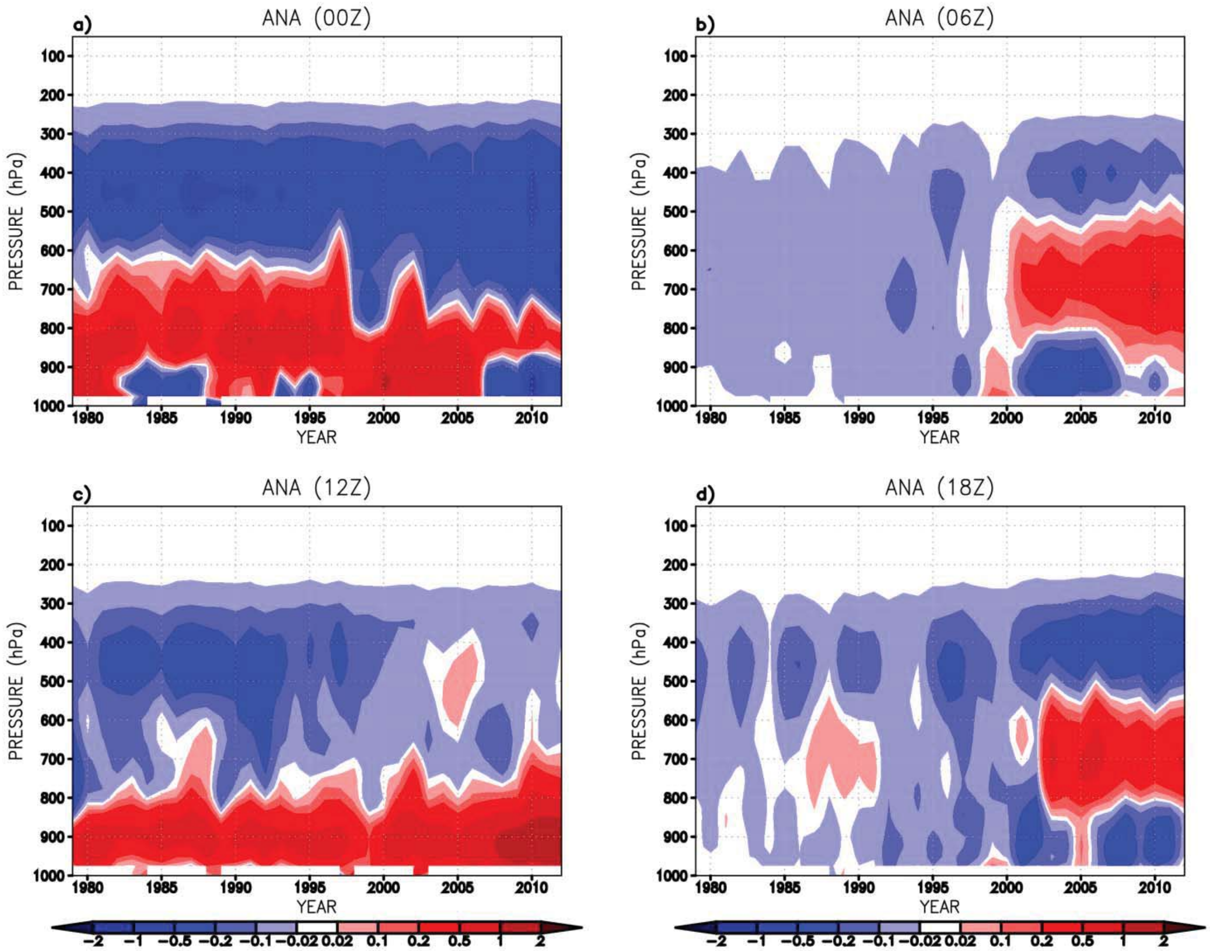

Figure 9 Time-height cross section of annual mean water analysis increment (g kg^{-1} day^{-1}) at a) 00Z, b) 06Z, c) 12Z, and d) 18Z over the central United States.

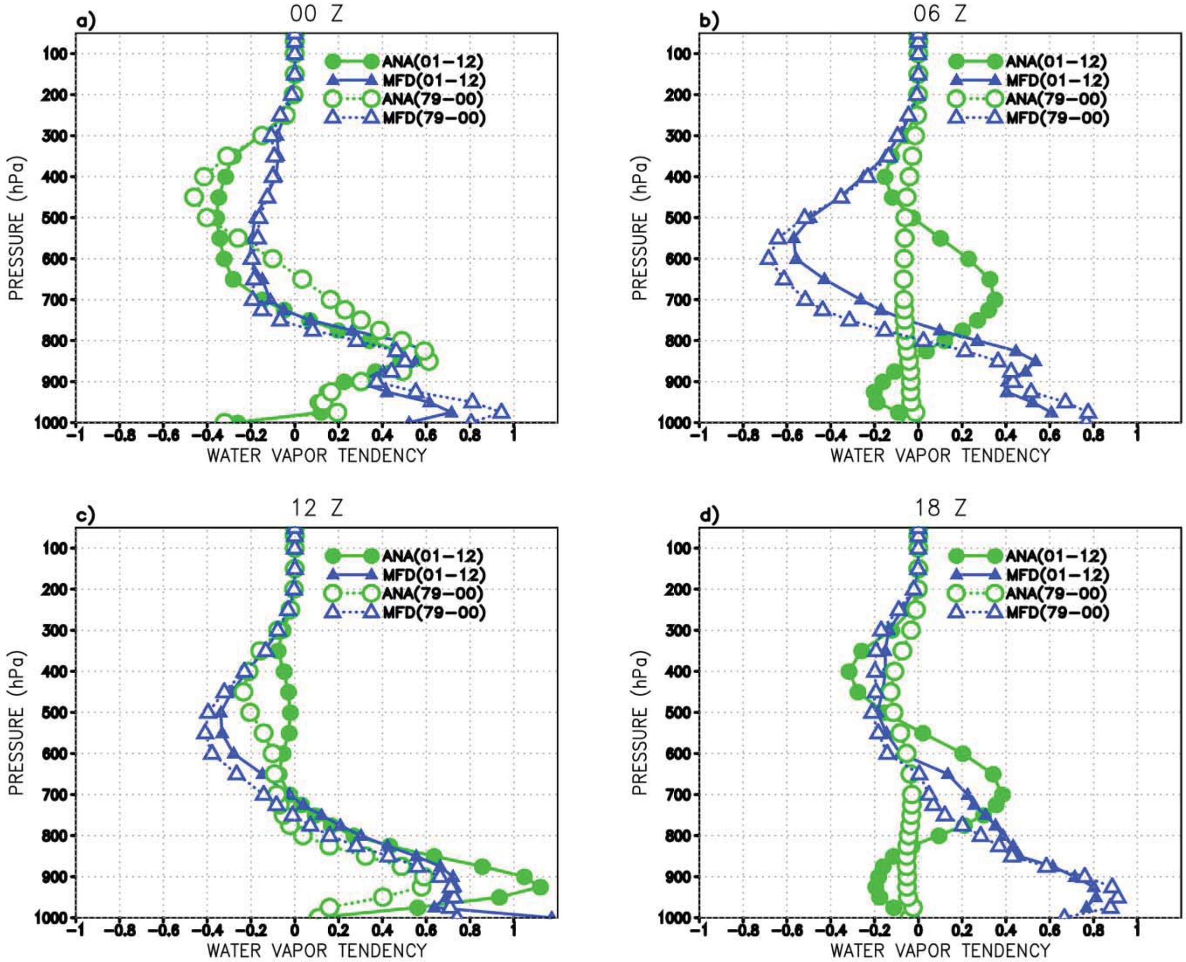

Figure 10 Vertical profiles of water vapor tendency ANA and MFD terms at a) 00Z, b) 06Z, c) 12Z, and d) 18Z over the central United States for period 1979-2000 (dot lines) and 2001-2012 (solid lines). All units are in g kg^{-1} day^{-1}.

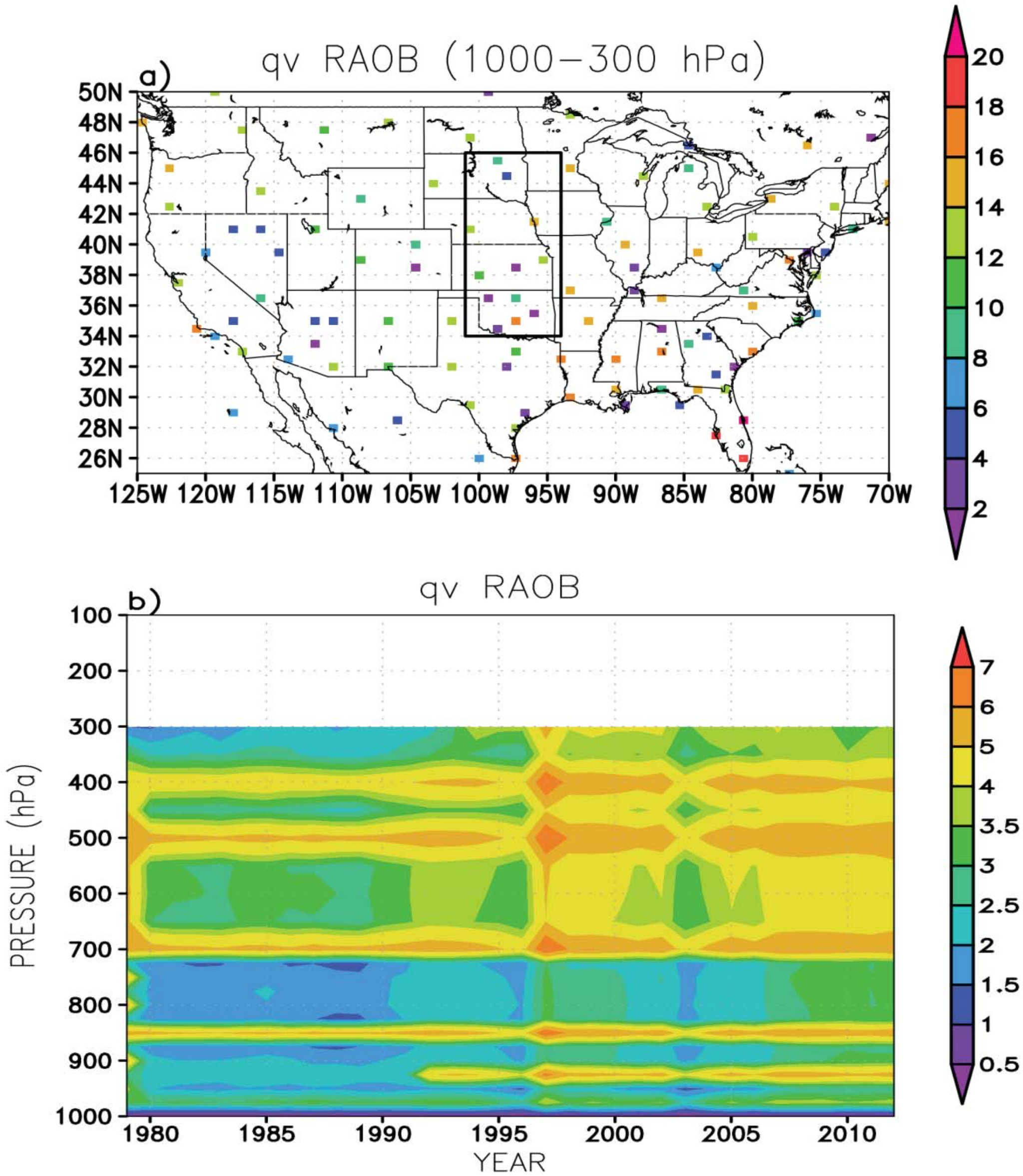

Figure 11 Annual mean number of observations (in thousands) for (a) RAOB stations in the United States from 1000 to 300 hPa (21 constant pressure levels) (b) time-height cross section over the Central United States box.

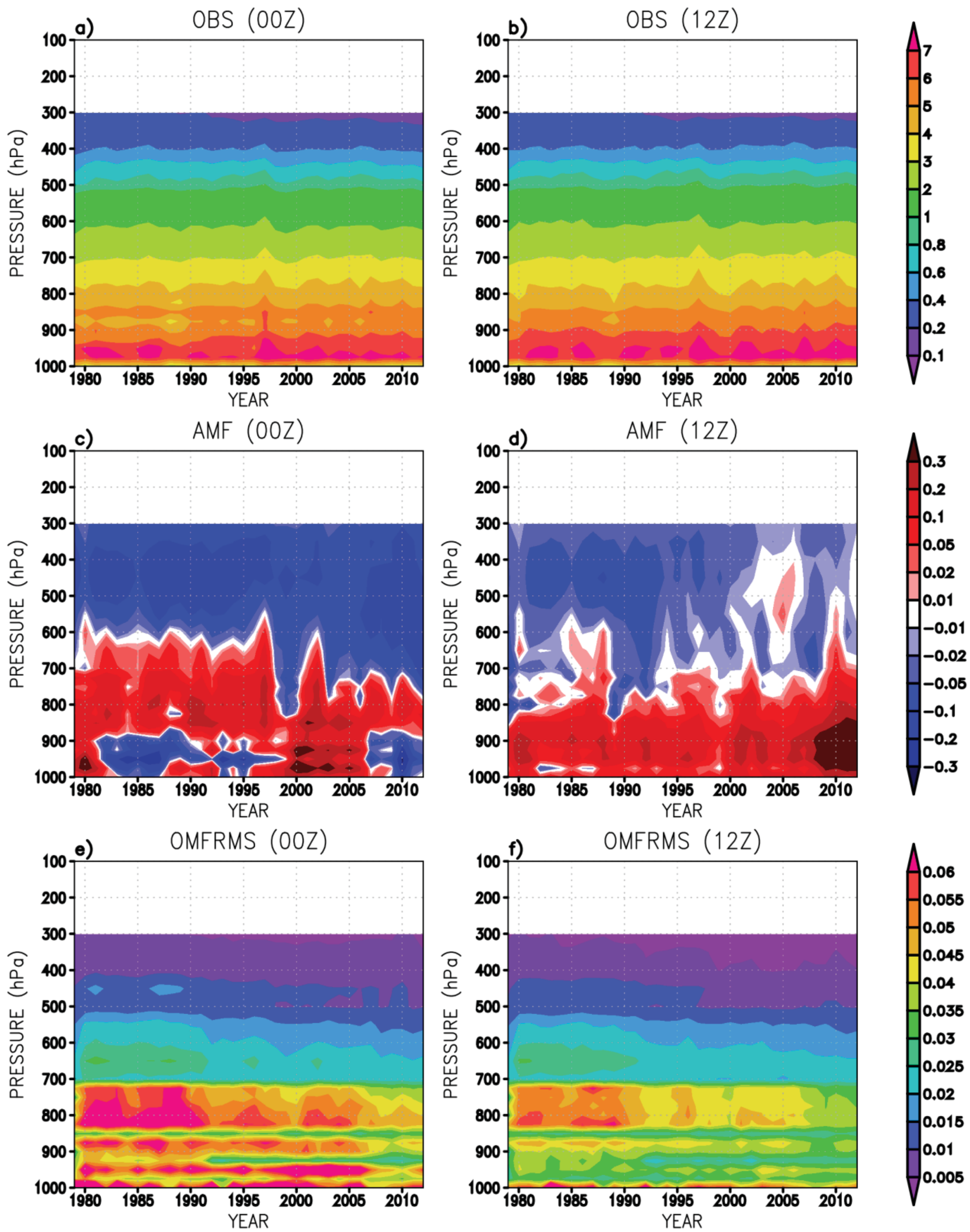

Figure 12 Annual mean water vapor mixing ratio observations (top), analysis departure (middle), and root mean square error of forecast departure (bottom) from RAOB over the central United States at 00Z (left) and 12Z (right). All units are in g kg^{-1}.

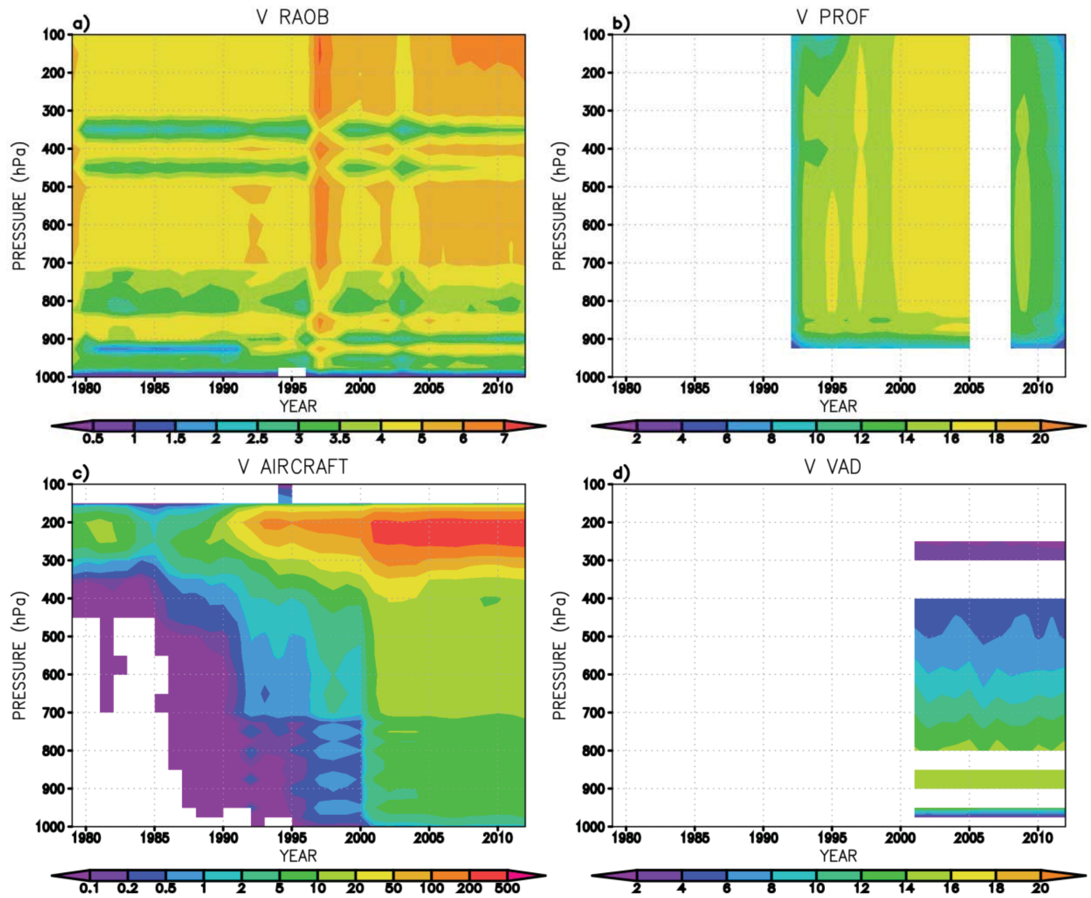

Figure 13 The annual number of meridional wind observations (in thousands) over the central United States for wind from a) Radiosonde, b) LIDAR profiler, c) Aircraft, d) VAD. A technical coding error lead for the MERRA input data lead to the wind profiler gap during 2006-2007.

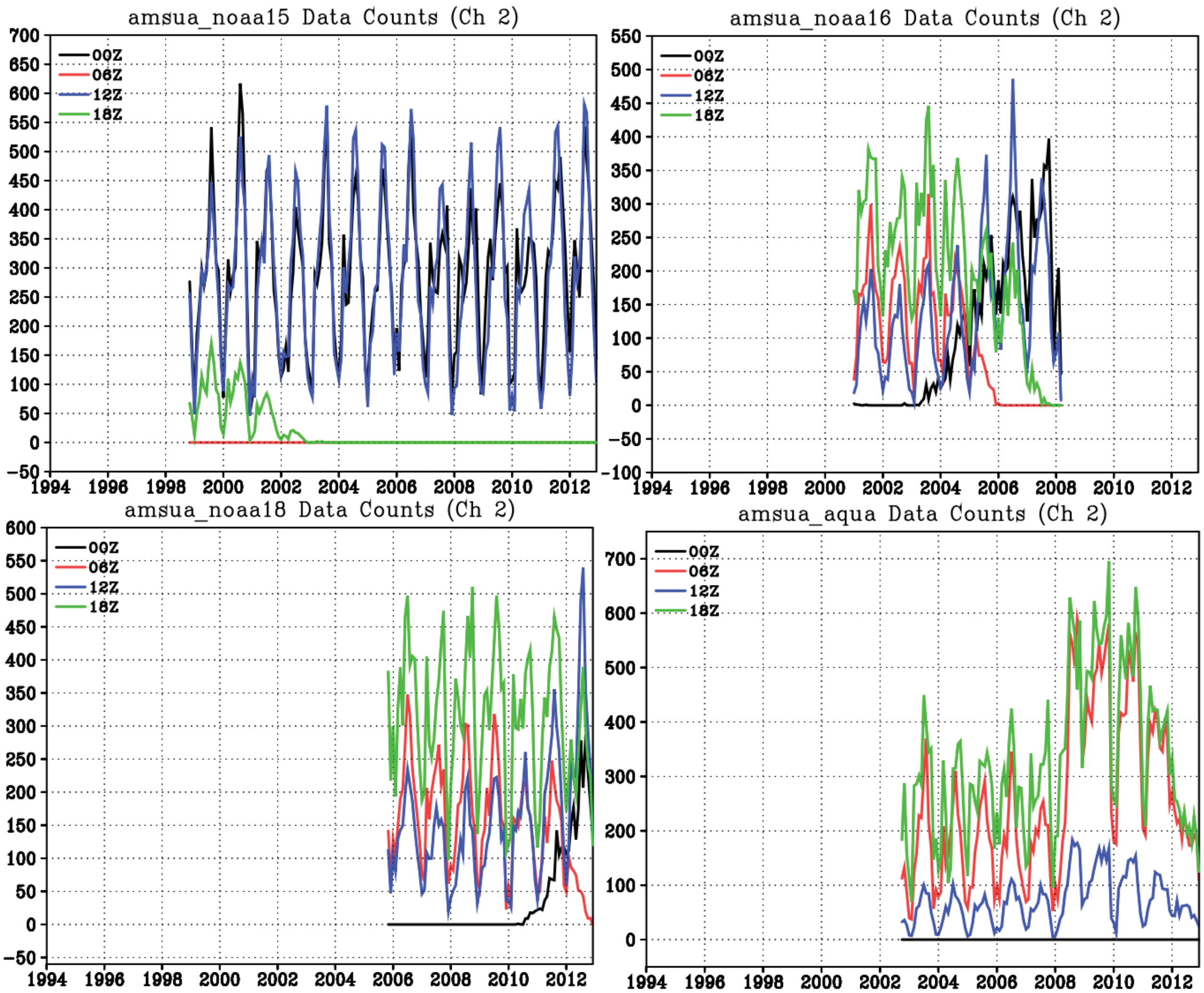

Figure 14 Monthly data count over the central US region for all platforms, NOAA15 (a), NOAA16 (b), NOAA18 (c), and Aqua (d), of AMSUA window channel 2, where each line indicates an analysis time. Lines may overlap, especially if no observations were present. These counts reflect the observations that were assimilated, and not the actual number of observations that may be available. Also, data thinning affects the number reported here.

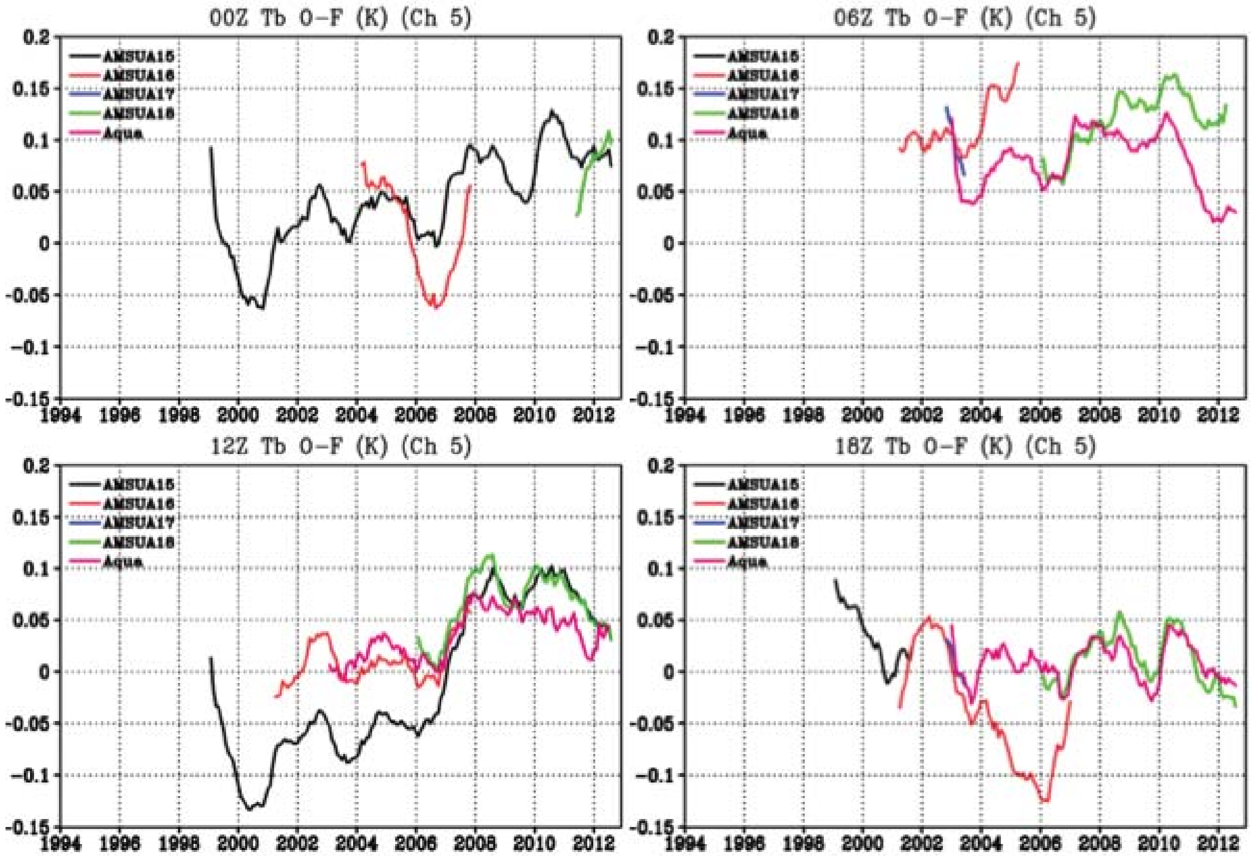

Figure 15 Monthly forecast departures (O-F) for AMSUA channel 5 brightness temperatures (K) over the central US region, separated by analysis time (a-d).

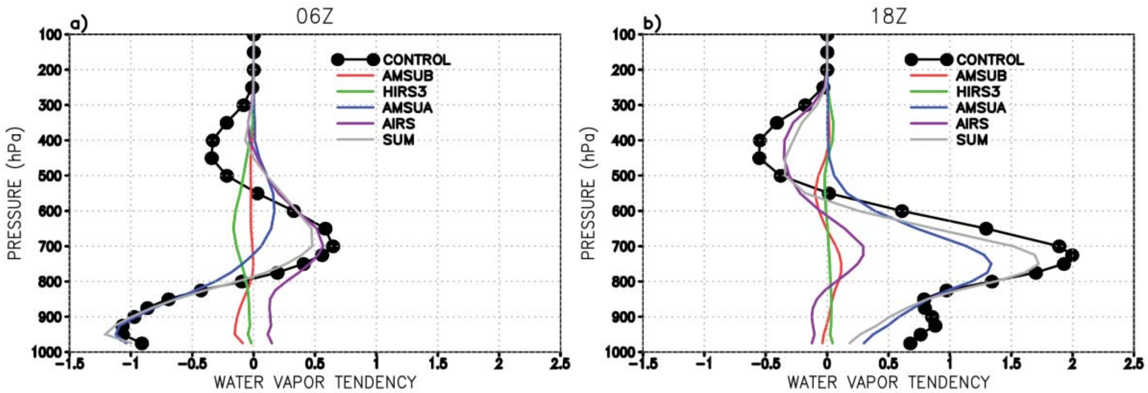

Figure 16 Contribution of selected instruments (AMSUA, AMSUB, HIRS3, and AIRS) to monthly mean ANA tendency (g kg-1 day-1) at (a) 06Z and (b) 18Z over the central US region in July 2005. Control experiment (CONTROL) has all observations as MERRA. The contribution of each instrument is the difference between the control experiment and each instrument's data withholding experiment. SUM is the summation of AMSUA, AMSUB, HIRS3, and AIRS.

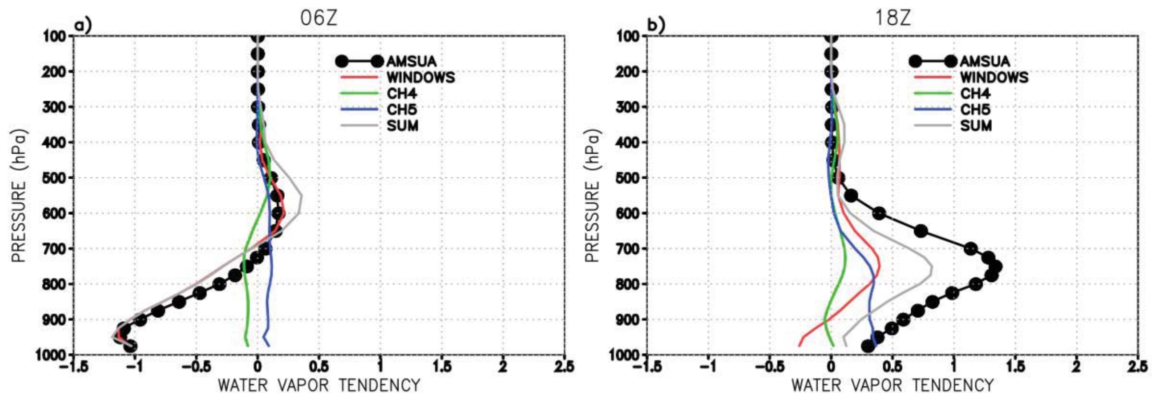

Figure 17 Contribution of AMSUA and its selected channels (window channels, channel 4 and channel 5) to monthly mean ANA tendency (g kg-1 day-1) at (a) 06Z and (b) 18Z over the central US region in July 2005. Window channel includes channel 1, 2, 3 and 15. The contribution of each channel is the difference between the control experiment and each channel's data withholding experiment. SUM is the summation of window channels, channel 4, and channel 5.